

Article

A Simple Method for the Evaluation of the Pulse Width of an Ultraviolet Femtosecond Laser Used in Two-Photon Ionization Mass Spectrometry

Tomoko Imasaka ^{1,*}, Akifumi Hamachi ², Tomoya Okuno ² and Totaro Imasaka ^{2,3}

¹ Laboratory of Chemistry, Graduate School of Design, Kyushu University, Fukuoka 815-8540, Japan

² Department of Applied Chemistry, Graduate School of Engineering, Kyushu University, Fukuoka 819-0395, Japan; hamachi.akifumi.967@s.kyushu-u.ac.jp (A.H.); tomoyawashere@yahoo.co.jp (T.O.); imasaka@cstf.kyushu-u.ac.jp (T.I.)

³ Division of Optoelectronics and Photonics, Center for Future Chemistry, Kyushu University, Fukuoka 819-0395, Japan

* Correspondence: imasaka@design.kyushu-u.ac.jp; Tel.: +81-92-553-4462

Academic Editor: Takayoshi Kobayashi

Received: 21 March 2016; Accepted: 29 April 2016; Published: 6 May 2016

Abstract: A simple method was proposed for on-site evaluation of the pulse width of an ultraviolet femtosecond laser coupled with a mass spectrometer. This technique was based on measurement of a two-photon ionization signal in mass spectrometry by translation of the prism in the pulse compressor of the femtosecond laser. The method was applied to optical pulses that were emitted at wavelengths of 267, 241, and 219 nm; the latter two pulses were generated by four-wave Raman mixing using the third harmonic emission of a Ti:sapphire laser (267 nm) in hydrogen gas. The measurement results show that this approach is useful for evaluation of the pulse width of the ultraviolet femtosecond laser used in mass spectrometry for trace analysis of organic compounds.

Keywords: pulse width; mass spectrometry; ionization; ultraviolet femtosecond laser

1. Introduction

Ultrashort laser pulses have been used successfully in a variety of applications including trace analysis of organic compounds [1]. Several techniques have been developed to measure the pulse width of the femtosecond laser, including autocorrelation (AC), spectral phase interferometry for direct electric field reconstruction (SPIDER), and frequency-resolved optical gating (FROG) [2]. Among these methods, the FROG technique is widely used and has several variations in its implementation. For example, second harmonic generation (SHG), polarization gating (PG), or self-diffraction (SD) can be used for the nonlinear optical effect. To expand the spectral domain to measure shorter pulse widths, third harmonic generation (THG), cross-correlation (X), and four-wave mixing (FWM) have all been used to date [3–6]. On the other hand, the pulse width of the UV femtosecond laser has been measured based on autocorrelation using a solid material, e.g., a CaF₂ plate, as a nonlinear optical device [7–10]. Moreover, the vacuum-ultraviolet (VUV) laser pulse has been measured by focusing it with a near-infrared (NIR) probe pulse into xenon to observe the cross-correlation signal of ionization [11–15]. However, the pulse duration would be changed by traveling even in ambient air from the location of the device used to perform the pulse width measurement to the point of application. Complex techniques such as attosecond streaking (AS) or FROG for complete reconstruction of attosecond bursts (FROG-CRAB) can be used to measure the pulse width in a vacuum chamber used for extreme ultraviolet (EUV) pulse generation [16,17]. However, these techniques are rather complicated for use in practical applications.

For simple on-site measurement of pulse widths, a device based on fringe-resolved autocorrelation (FRAC) was developed, which consisted of an interferometer and a time-of-flight mass spectrometer that was used as a two-photon-response detector to measure a non-resonant two-photon ionization signal [18–21]. However, the laser beam must be split into two parts and recombined after the interferometer, which reduces the laser pulse energy and then the sensitivity of the mass spectrometer. Also, the low-dispersion aluminum mirrors used in the interferometric system have substantial reflection losses in the deep-ultraviolet (DUV) region. In addition, the mass spectrometer must be operated for long periods, e.g., for periods of days, without maintenance to compare the data from repeated measurements obtained on the same day. Thus, it requires sufficient optical system stability for the pulse width measurements to be performed. In fact, we tried to measure an autocorrelation trace for a DUV pulse generated through several nonlinear optical processes combined in series, but the attempt was unsuccessful due to low pulse energy, poor beam quality, and instability of the laser pulse energy although performance of the laser was sufficient for application to mass spectrometry. Therefore, a simple and rugged instrument that does not contain an interferometer is highly desirable for evaluation of the widths of pulses from DUV femtosecond lasers. On the other hand, DUV femtosecond lasers have been used successfully for two-photon ionization applications in mass spectrometry [1]. Because the dispersion caused by the optical components or even by the ambient air cannot be negligible in the DUV region, a device such as a prism pair must be used for pulse compression in the laser system to generate a nearly-transform-limited pulse in the mass spectrometer [22]. It should be noted that a technique referred to as multiphoton intrapulse interference phase scan (MIIPS) or dispersion scan (d-can) has been reported, in which the SHG spectrum is measured by changing the dispersion in the beam path, e.g., by translating a wedge or prism, or changing the angle of a grating [23–29]. This method is useful for observing a two-dimensional display of the delay (dispersion) and the spectrum, allowing the full characterization of the chirp of the pulse. However, the use of a crystal for SHG limits the spectral range to the NIR-visible region and also makes the on-site measurement of the pulse width difficult.

In this study, we propose a simple method to evaluate the widths of pulses from a DUV femtosecond laser without use of an interferometer. This technique is based on measurement of a non-resonant two-photon ionization signal in mass spectrometry by translating the prism in the laser's pulse compressor. This method was applied to femtosecond optical pulses emitted at 241 and 219 nm, in addition to pulses emitted at 267 nm, which were generated by four-wave Raman mixing in hydrogen gas. The results obtained herein were compared with the transform-limited pulse widths that were calculated from the spectral bandwidths of the laser used in the experiments.

2. Theoretical Calculations

The electric field and intensity characteristics of an optical pulse with respect to time (t) can be assumed to have Gaussian profiles [2].

$$\tilde{E}(t) = E_0 e^{-at^2} e^{i(\omega t + bt^2)} \quad (1)$$

$$I(t) = |E_0|^2 e^{-2at^2} \quad (2)$$

where “ a ” is related to the pulse duration, Δt , as shown below, and “ b ” is a chirp parameter.

$$\sqrt{\frac{2\ln 2}{a}} \approx \Delta t \quad (3)$$

The second-order FRAC signal can be expressed as

$$I_{\text{FRAC}}^2(\tau) = \int_{-\infty}^{\infty} \left| (\tilde{E}(t - \tau) + \tilde{E}(t))^2 \right|^2 dt \quad (4)$$

where τ is the time delay between the two pulses in the interferometer [21]. This parameter can be set to zero because the beam is not separated in this study (*i.e.*, no interferometer is used), and this leads to Equation (5).

$$I_{\text{FRAC}}^2(\tau = 0) = \int_{-\infty}^{\infty} \left| (2\tilde{E}(t)) \right|^2 dt = 16 \int_{-\infty}^{\infty} \left| (\tilde{E}(t))^2 \right|^2 dt = 16 |E_0|^4 \int_{-\infty}^{\infty} e^{-4at^2} dt = 16A^2 \sqrt{\frac{a}{\pi}} \quad (5)$$

where the parameter, A , is defined as a pulse energy by the following equation.

$$\int_{-\infty}^{\infty} I(t) dt = |E_0|^2 \int_{-\infty}^{\infty} e^{-2at^2} dt = A \quad (6)$$

When the signal intensity becomes one half of this value via a chirp of the pulse,

$$I_{\text{FTL}}^2(\tau = 0) = 2I_{\text{CP}}^2(\tau = 0) \quad (7)$$

where I_{FTL}^2 and I_{CP}^2 are the signal intensities of the transform-limited and chirped pulses, respectively. The following equation is then obtained.

$$\sqrt{a_{\text{FTL}}} = 2\sqrt{a_{\text{CP}}} \quad (8)$$

where a_{FTL} and a_{CP} are the parameters that were calculated using Equation (3). Then,

$$\Delta t_{\text{CP}} = 2\Delta t_{\text{FTL}} \quad (9)$$

where Δt_{FTL} and Δt_{CP} are the pulse durations of the transform-limited and chirped pulses, respectively. The relationship between Δt_{CP} and Δt_{FTL} can be expressed as Equation (10) [21].

$$\Delta t_{\text{CP}} = \sqrt{(\Delta t_{\text{FTL}})^2 + \left(\frac{\varphi_2 \times 4\ln 2}{\Delta t_{\text{FTL}}} \right)^2} \quad (10)$$

where φ_2 is the group delay dispersion (GDD), which can be expressed as a product of the group velocity dispersion (GVD) determined using the Sellmeier equation [30,31] and the effective length of the optical material in the beam path, $\ell - \ell_0$ (see Figure 1a). Then,

$$\varphi_2 = GDD = GVD \times 2 \times (\ell - \ell_0) \quad (11)$$

where $\ell = (2 \tan 34^\circ) \times L$ for a Brewster prism used at approximately 250 nm. The factor of 2 in Equation (11) is multiplied due to a double pass of the beam in the prism. When the dispersion is canceled by a prism pair, $GDD = 0$ and $\ell_0 = (2 \tan 34^\circ) \times L_0$ where ℓ_0 and L_0 are the parameters of ℓ and L at which the dispersion is canceled (the two-photon ionization signal is maximal). A parameter of X can be defined as a displacement of the prism position from the optimum location that cancels the dispersion (*i.e.*, $GDD = 0$), then $X \equiv \ell - \ell_0$. When the intensity of the two-photon ionization signal decreases to one half of the maximum value, $L = L_{1/2}$ and then $X_{1/2} = L_{1/2} - \ell_0$. From Equations (9) and (10), Δt_{FTL} can then be rewritten as

$$\Delta t_{\text{FTL}} = \frac{\sqrt{4\ln 2}}{\sqrt[4]{3}} \sqrt{\varphi_2(X_{1/2})} \quad (12)$$

where $\varphi_2(X_{1/2})$ is the value of GDD at $X = X_{1/2}$. This equation suggests that the transform-limited pulse width can be calculated by measuring the parameter of $X_{1/2}$ in the experiment.

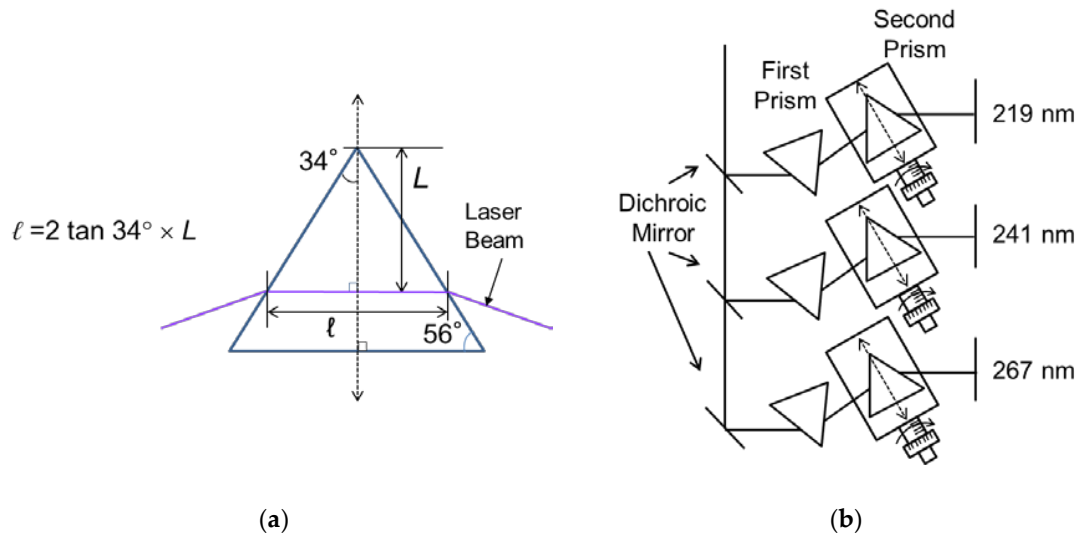


Figure 1. (a) Prism parameters; (b) configuration of the prisms in a pulse compressor. Dotted arrows show the direction of displacement of the prisms. The parameters, ℓ and L , are the path length of the laser beam in the prism and the distance from the top of the prism to the laser beam, respectively. The angle of the prism is specified in the figure. Three prisms in (b) can be manually translated by rotating the nobs of the differential micrometers independently.

The actual pulse width is, however, broadened by several reasons: (1) an initial laser pulse would be neither Gaussian-shaped nor transform-limited; (2) the laser pulse would be chirped even at the optimal prism position because of the third-order dispersion (TOD) of the fused silica of the prisms used for pulse compression; and (3) the pulse front would be deformed by mode-change and self-focusing during beam transmission in a hollow capillary filled with hydrogen gas (many hot spots were observed in the beam pattern). In order to take account of the deterioration of the laser beam, a parameter, α , can be introduced into Equation (12).

$$\Delta t_{\text{REAL}} = \frac{\sqrt{4 \ln 2}}{\sqrt[4]{3}} \sqrt{\alpha \times \varphi_2(X_{1/2})} \quad (13)$$

where Δt_{REAL} is the pulse width observed in the experiment and α is the parameter showing the deviation from the transform-limited pulse. When TOD is only a factor responsible for the distortion of the pulse, α can be written as $1 + \text{TOD}/\text{GVD}$ where

$$\text{GVD} = \frac{\lambda^3}{2\pi c^2} \frac{d^2 n}{d\lambda^2} \text{ and } \text{TOD} = -\left(\frac{\lambda}{2\pi c}\right)^2 \frac{1}{c} \left(3\lambda^2 \frac{d^2 n}{d\lambda^2} + \lambda^3 \frac{d^3 n}{d\lambda^3}\right) \quad (14)$$

Equations (11)–(13) lead to the following equations.

$$\text{When } \alpha = 1, \Delta t_{\text{FTL}} = \frac{\sqrt{16 \ln 2 \tan 34^\circ}}{\sqrt[4]{3}} \sqrt{\text{GVD} \times X_{1/2}} \quad (15)$$

$$\text{When } \alpha > 1, \Delta t_{\text{REAL}} = \frac{\sqrt{16 \ln 2 \tan 34^\circ}}{\sqrt[4]{3}} \sqrt{\text{GVD} \times \alpha \times X_{1/2}} = \Delta t_{\text{FTL}} \sqrt{\alpha} \quad (16)$$

As shown in Equation (16), the value of $X_{1/2}$ to be obtained for a transform-limited pulse is actually expanded to a value of $\alpha X_{1/2}$ in the experiment by some undesirable effects arising from additional chirps and deterioration of the laser pulse. The graph showing the relationship between Δt_{REAL} and $\alpha X_{1/2}$ is the same as that of Δt_{FTL} vs. $X_{1/2}$, as shown in Equations (15) and (16). As can be recognized from Equations (15) and (16), Δt_{REAL} is expanded by a factor of $\sqrt{\alpha}$ from Δt_{FTL} that can be

calculated from the spectral bandwidth of the laser beam. The parameter, α , can be calculated from the ratio of Δt_{REAL} and Δt_{FTL} , suggesting a degree of the deviation from the ideal transform-limited Gaussian pulse.

A train of ultrashort optical pulses is generated by superposition of the laser emissions, which are phase-locked to each other. In this study, three beams, *i.e.*, 9ω (267 nm), 10ω (241 nm), and 11ω (219 nm), where $\omega = 4155 \text{ cm}^{-1}$, were superimposed and were then used as one of the test beams. The spectral width, $\Delta\omega_n$, and the parameter, a_n , where $n = 1, 2, 3$, for each beam, were assumed to be $\Delta\omega_1 = \Delta\omega_2 = \Delta\omega_3 = \Delta\omega$ and $a_1 = a_2 = a_3 = a$ for the purposes of this study. A train of ultrashort pulses is formed under these conditions if the three emission lines are phase locked. Thus, the phase locking expected to occur during the process of four-wave Raman mixing, can be confirmed by comparing the experimental data with the simulation results. The GDD can then be expressed as follows [2,21].

$$\varphi_2 \equiv GDD = \frac{b}{2(a^2 + b^2)} \quad (17)$$

$$\frac{a}{2(a^2 + b^2)} = \ln 2 \left(\frac{2}{\Delta\omega} \right)^2, b = \frac{(\Delta\omega)^2 \times GDD}{2(\Delta t)^2} \quad (18)$$

When the laser emissions are phase-locked together, $I_{\text{FRAC}}^2(\tau = 0)$ can be written as

$$I_{\text{FRAC}}^2(\tau = 0) = \int_{-\infty}^{\infty} \left| (2(\tilde{E}_1(t) + \tilde{E}_2(t) + \tilde{E}_3(t)))^2 \right|^2 dt \quad (19)$$

By assuming that $E_{0,1} = E_{0,2} = E_{0,3} = 1$ for simplicity,

$$I_{\text{FRAC}}^2(\tau = 0) = 16 \int_{-\infty}^{\infty} \left| (e^{-a_1 t^2} e^{i(\omega_1 t + b_1 t^2)} + e^{-a_2 t^2} e^{i(\omega_2 t + b_2 t^2)} + e^{-a_3 t^2} e^{i(\omega_3 t + b_3 t^2)})^2 \right|^2 dt \quad (20)$$

It should be noted that the three transform-limited pulses are assumed to be superimposed in-phase without any chirp in Equation (20). In contrast, when the laser emissions are not phase-locked to each other (*i.e.*, they are randomly phased), $I_{\text{FRAC}}^2(\tau = 0)$ can then be expressed as

$$I_{\text{FRAC}}^2(\tau = 0) = \int_{-\infty}^{\infty} \left| (2e^{-a_1 t^2} e^{i(\omega_1 t + b_1 t^2)})^2 \right|^2 dt + \int_{-\infty}^{\infty} \left| (2e^{-a_2 t^2} e^{i(\omega_2 t + b_2 t^2)})^2 \right|^2 dt + \int_{-\infty}^{\infty} \left| (2e^{-a_3 t^2} e^{i(\omega_3 t + b_3 t^2)})^2 \right|^2 dt \quad (21)$$

The spectral width can be assumed to be $\Delta\omega = 2\omega$, although the actual spectral shape is far beyond a Gaussian profile. The experimental data can then be compared with the data calculated using Equations (20) and (21).

3. Experimental

An optical parametric amplifier (OPA, OPerA-Solo, <50 fs, Coherent, Inc., Santa Clara, CA, USA) was pumped by a Ti:sapphire laser (800 nm, 35 fs, 4 mJ, 1 kHz, Elite, Coherent, Santa Clara, CA, USA). The beam of the Ti:sapphire laser that remained for mixing with the OPA output was used for third harmonic generation (267 nm). The remaining fundamental beam (800 nm) and the signal beam of the OPA (1200 nm) were spatially and temporally superimposed on each other and were focused into a hollow capillary filled with hydrogen gas for vibrational molecular modulation. The third harmonic emission (267 nm) was then focused into the hollow capillary to provide frequency modulation and generate vibrational Raman emissions at 241 and 219 nm. The three-color beam (267, 241, 219 nm) was separated into three individual beams using three dielectric mirrors (Sigma Koki, Tokyo, Japan) placed in series, as shown in Figure 1b. The laser beams passed through three pairs of prisms for pulse compression. The beams were then reflected by a pair of roof mirrors and were

recombined into a single beam using the dielectric mirrors. The three-color beam was then focused by a concave mirror into a molecular beam in a mass spectrometer (Hikari Gijyutsu Corp., Fukuoka, Japan). The energy of each pulse measured in front of the mass spectrometer was *ca.* 1 μ J. In the experiment, 1,4-dioxane was introduced into the mass spectrometer for recording of a non-resonant two-photon ionization signal [20]. The signal intensity was measured by translating the second prism to alter the positive dispersion in the compressor. The parameter $X_{1/2}$ was determined to be the half width at half maximum of the observed data. The spectral bandwidth of the laser was measured using a spectrometer (Maya2000pro, spectral resolution 1.5 nm, Ocean Optics, Dunedin, FL, USA), the resolution of which was calibrated using a mercury lamp (Ocean Optics, Dunedin, FL, USA) at 254 nm.

4. Results and Discussion

4.1. Calculations

Figure 2 shows the dependence of Δt_{REAL} on $\alpha X_{1/2}$ (or Δt_{FTL} on $X_{1/2}$), which was calculated in the range from 2ω to 16ω ($\omega = 4155 \text{ cm}^{-1}$) using Equation (16). Because the dispersion increases at higher frequencies, the pulse width increases even at the same value of $\alpha X_{1/2}$. For example, when $\alpha X_{1/2} = 1 \text{ mm}$, the pulse width becomes 5.0 fs at 2ω and 95 fs at 16ω . Another example would be $\alpha X_{1/2} = 10 \text{ mm}$, providing pulse widths of 16 fs at 2ω and 300 fs at 16ω . Therefore, the pulse width can be evaluated based on the observed data to show the dependence of the two-photon ionization signal on the displacement (X) of the second prism in the pulse compressor.

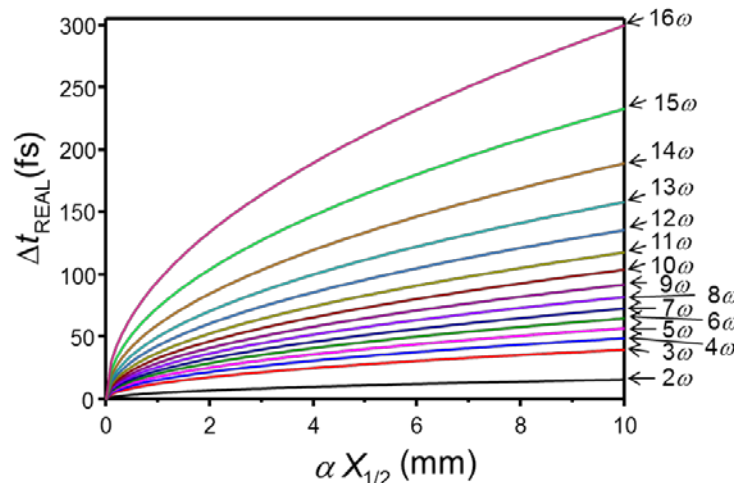


Figure 2. Calculated dependence of the parameter, Δt_{REAL} , on the parameter, $\alpha X_{1/2}$. The laser frequency, $n\omega$, is shown in the figure, where n and ω are the order of Raman sidebands and the Raman shift frequency of molecular hydrogen ($\omega = 4155 \text{ cm}^{-1}$), respectively. The definitions of the parameters, Δt_{REAL} and $\alpha X_{1/2}$, are given in the text.

4.2. Pulse Width Evaluation

Figure 3 shows the dependence of the signal intensities measured as a function of the prism displacement, X , for laser beams emitted at 9ω (=267 nm), 10ω (=241 nm), and 11ω (=219 nm). Because $\alpha X_{1/2} = 4.9 \text{ mm}$ at 9ω , the pulse width, Δt_{REAL} , can be calculated to be 64 fs from the data shown in Figure 2. For the values of $\alpha X_{1/2} = 5.6 \text{ mm}$ at 10ω and 1.7 mm at 11ω , the corresponding values of Δt_{REAL} can be calculated to be 78 and 49 fs, respectively. The spectral bandwidth was measured using a spectrometer, and the estimated values were *ca.* 3.3, 2.9, and 2.5 nm after calibration of the resolution (1.5 nm) of the spectrometer at 9ω , 10ω , and 11ω , respectively. From the relationship of $\Delta t \times \Delta\nu \geq k$ (where $k = 0.441$ for a Gaussian pulse), Δt_{FTL} can be calculated to be 36, 34, and 35 fs at 9ω , 10ω , and 11ω , respectively. The parameter, α , can then be calculated to *ca.* 3.2, 5.3, and 2.0 for 9ω , 10ω , and 11ω ,

respectively. These results suggest that the anti-Stokes beam has the shortest pulse width among them and has a slightly (1.4 times) larger pulse width than the width expected for a transform-limited pulse.

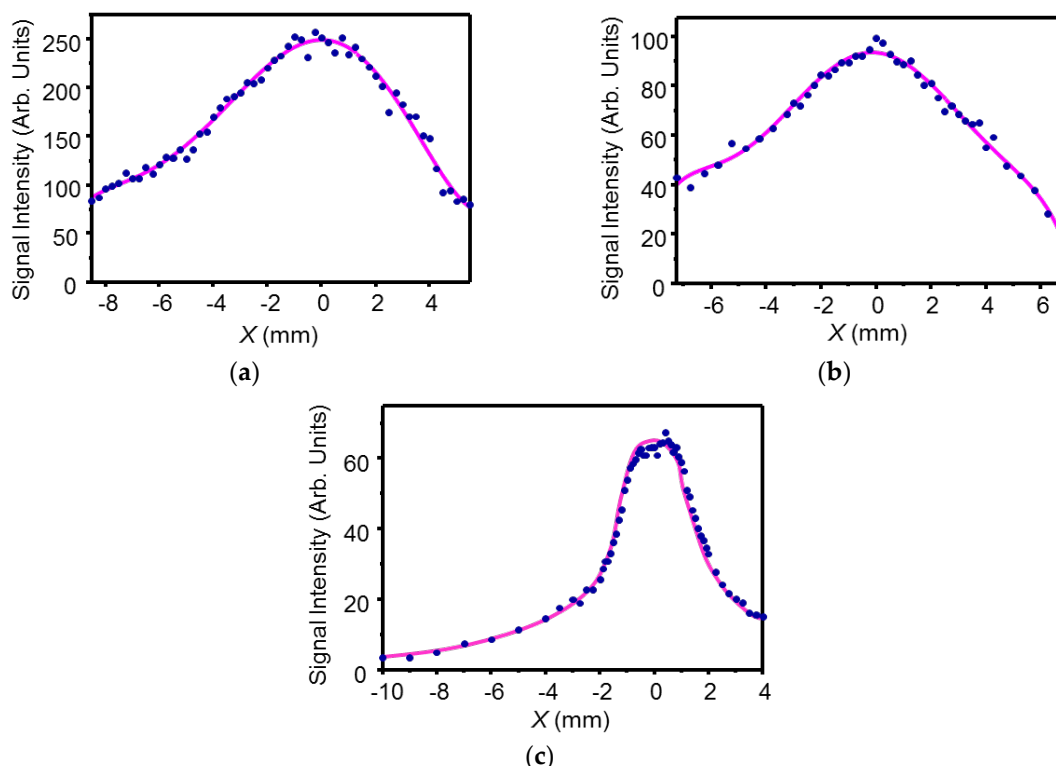


Figure 3. Observed dependence of the signal intensity, $I_{\text{FRAc}}^2 (\tau = 0)$, on the parameter, X . The dots in the figure are the observed data, and a solid curve is a guide to the eye. The parameter of $X_{1/2}$ can be obtained by calculating the half width at the half maximum of the signal peak. Laser operating wavelengths: (a) 267; (b) 241; and (c) 219 nm.

While the spectral profile of the three-color beam composed from the three spectral lines (267, 241, 219 nm) was far beyond the Gaussian shape, the presented technique was applied to this type of beam on a trial basis. The predicted results were calculated for two cases: (1) where the phases of the emissions are random; and (2) where the emission lines are phase-locked. In the former case, a broad band profile was obtained, as shown in Figure 4a, in which $\alpha X_{1/2} = 2.8$ mm. In the latter case, a very sharp peak, *i.e.*, $\alpha X_{1/2} = 0.015$ mm, was obtained, as shown in Figure 4b. The experimental data shown in Figure 4c consisted of two components, where one is a sharp peak ($\alpha X_{1/2} = 0.12$ mm) at the center, and the other is a broad band observed as a pedestal. It should be noted that the signal intensity was highly sensitive to the positions of the second prisms in the vicinity of the maximum value, and that this result was obtained by carefully translating these prisms simultaneously after critical optimization of their positions.

It is possible to consider that a sharp peak would arise from the phase-locked components while another would arise from the phase-random components. The former peak width (0.12 mm), corresponding to a pulse width of 11 fs, was apparently broader than the theoretically predicted value (0.015 mm), corresponding to a pulse width of 4.0 fs. This discrepancy is likely to arise from insufficient precision in phase control of the three emissions, during which the prisms were moved simultaneously using translation stages equipped with manually driven differential micrometers (see Figure 1b). Another explanation for the discrepancy, and the appearance of the pedestal, could be the spectral phase and amplitude fluctuations between the three pulses used in this study [32].

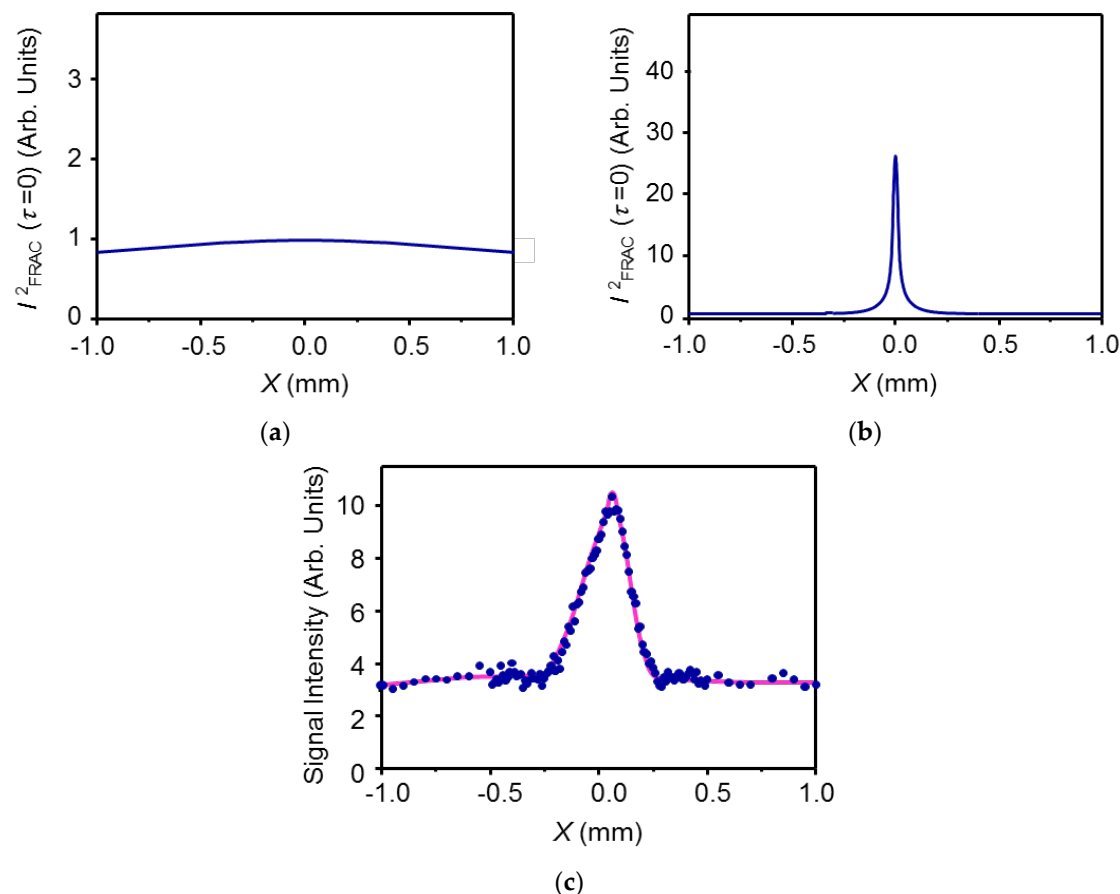


Figure 4. Calculated dependence of the parameter, I^2_{FRAC} ($\tau = 0$), on the parameter, X : (a) random phase; and (b) phase-locked; (c) Observed dependence of the signal intensity, I^2_{FRAC} ($\tau = 0$), on the parameter, X . The parameter of $X_{1/2}$ can be obtained by calculating the half width at the half maximum of the signal peak. In this case, a three-color beam emitting at 267, 241, and 219 nm was introduced into the molecular beam in the mass spectrometer.

5. Conclusions

A simple method for evaluation of the widths of pulses from a UV femtosecond laser was proposed that was based on measurement of a two-photon ionization signal by translation of the second prism in the laser's pulse compressor. The pulse widths that were observed experimentally showed reasonably good agreement with the values that were calculated from the spectral bandwidths, which were measured using a spectrometer. The method presented here could be applied to lasers with shorter pulse widths by using a prism with lower TOD, e.g., a prism made of CaF_2 or MgF_2 . The main advantage of this method is the minimal loss of pulse energy during measurement of the pulse width. Therefore, this technique can be used to evaluate the widths of pulses from the UV femtosecond laser that is used as an ionization source in mass spectrometry for practical trace analysis.

Acknowledgments: This research was supported by Grants-in-Aid from the Japan Society for the Promotion of Science (JSPS) KAKENHI (Grant Nos. 23245017, 24510227, 26220806, and 15K01227).

Author Contributions: Totaro Imasaka conceived and designed the experiments and theory; Tomoko Imasaka designed the theory; Akifumi Hamachi and Tomoya Okuno performed the experiments; All authors analyzed the data; Totaro Imasaka contributed reagents/materials/analysis tools; Totaro Imasaka and Tomoko Imasaka wrote the paper.

Conflicts of Interest: The authors declare no conflict of interest.

References

1. Imasaka, T. Gas chromatography/multiphoton ionization/time-of-flight mass spectrometry using a femtosecond laser. *Anal. Bioanal. Chem.* **2013**, *405*, 6907–6912. [CrossRef] [PubMed]
2. Trebino, R. *Frequency-Resolved Optical Gating: The Measurement of Ultrashort Laser Pulses*; Kluwer Academic Publishers: Boston, MA, USA, 2002.
3. Chadwick, R.; Spahr, E.; Squier, J.A.; Durfee, C.G.; Walker, B.C.; Fittinghoff, D.R. Fringe-free, background-free, collinear third-harmonic generation frequency-resolved optical gating measurements for multiphoton microscopy. *Opt. Lett.* **2006**, *31*, 3366–3368. [CrossRef] [PubMed]
4. Meshulach, D.; Barad, Y.; Silberberg, Y. Measurement of ultrashort optical pulses by third-harmonic generation. *J. Opt. Soc. Am. B* **1997**, *14*, 2122–2125. [CrossRef]
5. Nomura, Y.; Shirai, H.; Ishii, K.; Tsurumachi, N.; Voronin, A.A.; Zheltikov, A.M.; Fuji, T. Phase-stable sub-cycle mid-infrared conical emission from filamentation in gases. *Opt. Express* **2012**, *20*, 24741–24747. [CrossRef] [PubMed]
6. Shverdin, M.Y.; Walker, D.R.; Yavuz, D.D.; Yin, G.Y.; Harris, S.E. Generation of a single-cycle optical pulse. *Phys. Rev. Lett.* **2005**, *94*, 033904. [CrossRef] [PubMed]
7. Tzankov, P.; Steinkellner, O.; Zheng, J.; Mero, M.; Freyer, W.; Husakou, A.; Babushkin, I.; Herrmann, J.; Noack, F. High-power fifth-harmonic generation of femtosecond pulses in the vacuum ultraviolet using a Ti:sapphire laser. *Opt. Express* **2007**, *15*, 6389–6395. [CrossRef]
8. Homann, C.; Lang, P.; Riedle, E. Generation of 30 fs pulses tunable from 189 to 240 nm with an all-solid-state setup. *J. Opt. Soc. Am. B* **2012**, *29*, 2765–2769. [CrossRef]
9. Zuo, P.; Fuji, T.; Horio, T.; Adachi, S.; Suzuki, T. Simultaneous generation of ultrashort pulses at 158 and 198 nm in a single filamentation cell by cascaded four-wave mixing in Ar. *Appl. Phys. B* **2012**, *108*, 815–819. [CrossRef]
10. Mero, M.; Zheng, J. Femtosecond optical parametric converter in the 168–182-nm range. *Appl. Phys. B* **2012**, *106*, 37–43. [CrossRef]
11. Trushin, S.A.; Fuss, W.; Kosma, K.; Schmid, W.E. Widely tunable ultraviolet sub-30-fs pulses from supercontinuum for transient spectroscopy. *Appl. Phys. B* **2006**, *85*, 1–5. [CrossRef]
12. Trushin, S.A.; Kosma, K.; Fuß, W.; Schmid, W.E. Sub- 10-fs supercontinuum radiation generated by filamentation of few-cycle 800 nm pulses in argon. *Opt. Lett.* **2007**, *32*, 2432–2434. [CrossRef] [PubMed]
13. Kosma, K.; Trushin, S.A.; Schmid, W.E.; Fuß, W. Vacuum ultraviolet pulses of 11 fs from fifth-harmonic generation of a Ti:sapphire laser. *Opt. Lett.* **2008**, *33*, 723–725. [CrossRef] [PubMed]
14. Beutler, M.; Ghotbi, M.; Noack, F. Generation of intense sub-20-fs vacuum ultraviolet pulses compressed by material dispersion. *Opt. Lett.* **2011**, *36*, 3726–3728. [CrossRef] [PubMed]
15. Ghotbi, M.; Trabs, P.; Beutler, M.; Noack, F. Generation of tunable sub-45 femtosecond pulses by noncollinear four-wave mixing. *Opt. Lett.* **2013**, *38*, 486–488. [CrossRef] [PubMed]
16. Wirth, A.; Hassan, M.T.; Grguraš, I.; Gagnon, J.; Moulet, A.; Luu, T.T.; Pabst, S.; Santra, R.; Alahmed, Z.A.; Azzeer, A.M.; et al. Synthesized light transients. *Science* **2011**, *334*, 195–200. [CrossRef] [PubMed]
17. Mairesse, Y.; Quéré, F. Frequency-resolved optical gating for complete reconstruction of attosecond bursts. *Phys. Rev. A* **2005**, *71*, 011401. [CrossRef]
18. Zaitsu, S.; Miyoshi, Y.; Kira, F.; Yamaguchi, S.; Uchimura, T.; Imasaka, T. Interferometric characterization of ultrashort deep ultraviolet pulses using a multiphoton ionization mass spectrometer. *Opt. Lett.* **2007**, *32*, 1716–1718. [CrossRef] [PubMed]
19. Imasaka, T.; Imasaka, T. Searching for a molecule with a wide frequency domain for non-resonant two-photon ionization to measure the ultrashort optical pulse width. *Opt. Commun.* **2012**, *285*, 3514–3518. [CrossRef]
20. Okuno, T.; Imasaka, T.; Kida, Y.; Imasaka, T. Autocorrelator for measuring an ultrashort optical pulse width in the ultraviolet region based on two-photon ionization of an organic compound. *Opt. Commun.* **2014**, *310*, 48–52. [CrossRef]
21. Imasaka, T.; Okuno, T.; Imasaka, T. The search for a molecule to measure an autocorrelation trace of the second/third harmonic emission of a Ti:sapphire laser based on two-photon resonant excitation and subsequent one-photon ionization. *Appl. Phys. B* **2013**, *113*, 543–549. [CrossRef]
22. Hamachi, A.; Okuno, T.; Imasaka, T.; Kida, Y.; Imasaka, T. Resonant and nonresonant multiphoton ionization processes in the mass spectrometry of explosives. *Anal. Chem.* **2015**, *87*, 3027–3031. [CrossRef] [PubMed]

23. Lozovoy, V.V.; Pastirk, I.; Dantus, M. Multiphoton intrapulse interference. IV. Ultrashort laser pulse spectral phase characterization and compensation. *Opt. Lett.* **2004**, *29*, 775–777. [[CrossRef](#)] [[PubMed](#)]
24. Xu, B.; Gunn, J.M.; Dela Cruz, J.M.; Lozovoy, V.V.; Dantus, M. Quantitative investigation of the multiphoton intrapulse interference phase scan method for simultaneous phase measurement and compensation of femtosecond laser pulses. *J. Opt. Soc. Am. B* **2006**, *23*, 750–759. [[CrossRef](#)]
25. Coello, Y.; Lozovoy, V.V.; Gunaratne, T.C.; Xu, B.; Borukhovich, I.; Tseng, C.-H.; Weinacht, T.; Dantus, M. Interference without an interferometer: A different approach to measuring, compressing, and shaping ultrashort laser pulses. *J. Opt. Soc. Am. B* **2008**, *25*, A140–A150. [[CrossRef](#)]
26. Lozovoy, V.V.; Xu, B.; Coello, Y.; Dantus, M. Direct measurement of spectral phase for ultrashort laser pulses. *Opt. Express* **2008**, *16*, 592–597. [[CrossRef](#)] [[PubMed](#)]
27. Miranda, M.; Fordell, T.; Arnold, C.; L’Huillier, A.; Crespo, H. Simultaneous compression and characterization of ultrashort laser pulses using chirped mirrors and glass wedges. *Opt. Express* **2012**, *20*, 688–697. [[CrossRef](#)] [[PubMed](#)]
28. Miranda, M.; Arnold, C.L.; Fordell, T.; Silva, F.; Alonso, B.; Weigand, R.; L’Huillier, A.; Crespo, H. Characterization of broadband few-cycle laser pulses with the d-scan technique. *Opt. Express* **2012**, *20*, 18732–18743. [[CrossRef](#)] [[PubMed](#)]
29. Loriot, V.; Gitzinger, G.; Forget, N. Self-referenced characterization of femtosecond laser pulses by chirp scan. *Opt. Express* **2013**, *21*, 24879–24893. [[CrossRef](#)] [[PubMed](#)]
30. Sellmeier, W. Theory of anomalous light dispersion. *Ann. Phys. Chem.* **1871**, *143*, 271.
31. Malitson, I.H. Interspecimen comparison of refractive index of fused silica. *J. Opt. Soc. Am.* **1965**, *55*, 1205–1209. [[CrossRef](#)]
32. Rasskazov, G.; Lozovoy, V.V.; Dantus, M. Spectral amplitude and phase noise characterization of titanium-sapphire lasers. *Opt. Express* **2015**, *23*, 23597–23602. [[CrossRef](#)] [[PubMed](#)]



© 2016 by the authors; licensee MDPI, Basel, Switzerland. This article is an open access article distributed under the terms and conditions of the Creative Commons Attribution (CC-BY) license (<http://creativecommons.org/licenses/by/4.0/>).